Recent Developments in Direct-UV-Written Planar Waveguides, Gratings, Sensors, and Substrates

F.R. Mahamd Adikan, J.C. Gates, A.S. Webb, H.E. Major, C. Holmes, M. A. G. Ramirez, B. D. Snow, D. O. Kundys, C.B.E. Gawith, P.G.R. Smith
Optoelectronics Research Centre, University of Southampton, Highfield SO17 1BJ United Kingdom

Abstract: *We present our recent developments in direct-UV-written integrated optical devices, based on applications in telecommunications, material characterisation, and optical sensing. The inherent advantages of this channel definition technique over traditional etching based approaches are reiterated and demonstrated in the production of small angle, low loss X-couplers with negligible polarisation dependence. Interfering two focussed UV spots also provides us with the capability to simultaneously define a channel waveguide and Bragg grating, opening new device and application opportunities. Such structures provide a method to quantify the photosensitivity effects observed in conventional multilayer substrates, and assess the core uniformity of a novel 'flat-fibre' format recently developed within the ORC. We will also discuss electrically tuned Bragg gratings via liquid crystal overlayers, displaying a dynamic range in excess of 100GHz for use in dynamic optical networks.*

Introduction

Direct UV writing is planar lightwave circuit fabrication technique with enormous potential for the development of novel integrated optical devices and applications. Based on the refractive index change induced by a scanning UV beam, this technique allows channel waveguide structures to be literally 'drawn' into photosensitive materials without the need for photolithography, etching, or expensive cleanroom processing.

Historically, the concept of UV-based waveguide definition was introduced by Chandross et al. in 1974 [1], who produced 4μm optical waveguides in doped polymer films with a 364nm laser. Referring to the process as 'photolocking', Chandross commented that the 'smooth interfaces and low optical losses' would provide a route to avoid the characteristic edge roughness induced by solvent development or sputtering. For integrated optical applications, direct UV writing in silica-on-silicon was first reported by Svalgaard et al. in 1994 who demonstrated buried single-mode channel waveguides in germanium-doped silica films with a refractive index increase of 10^{-3} [2]. This was followed by work on practical devices such as directional couplers and power splitters in 1997 [3, 4] displaying losses of ~0.2dB.

The first reported experimental work from the Smith group at the ORC of Southampton University was in 2002 when Gawith reported direct-UV-written buried channel waveguide lasers in direct-bonded glass [5]. This was quickly followed by Emmerson, who described a more advanced 'Direct Grating Writing' technique for the simultaneous definition of channel waveguides and Bragg gratings via the interference of two focussed UV spots (Fig.1) [6]. Since then, direct UV writing at the ORC has primarily developed towards the realisation of planar Bragg-grating-based devices for real-world integrated optical applications, such as telecommunications and bio/chemical sensing.

Presented here is an overview of some of our recent developments in direct UV writing, and the many emerging applications discovered from this versatile technology. Specific examples include X-couplers for dense optical networks, and a subsequent study on photosensitivity and local control of refractive index. The use of direct UV writing as a characterisation tool is discussed during the introduction of a novel 'flat-fibre' extended-length planar substrate material developed for distributed lab-on-a-chip applications. Also described is a new Bragg grating device that can be electrically tuned over more than four 25GHz-spaced wavelength division multiplexed (WDM) channels by means of index modification of a liquid crystal layer. Finally, we aim to highlight UV writing technologies that we believe may benefit other areas, such as bio/chemical sensing and the automotive industry.

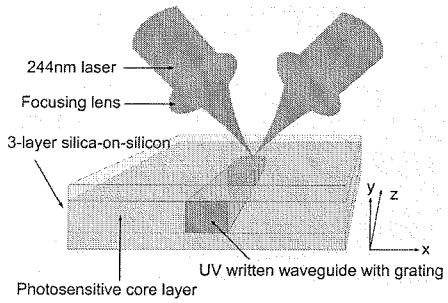

Fig: 1 Schematic diagram of simultaneous channel and grating definition via Direct Grating Writing

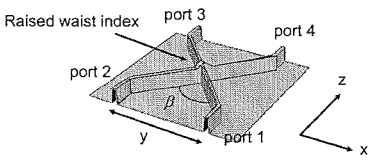

Launch port	Measured power	
	Through, $P_=$	Coupled, P_x
port 1	port 3	port 4
port 2	port 4	port 3

Fig: 2 Schematic diagram of an X-coupler showing the UV induced refractive index structure. Note the raised index close to the overlap region (β = crossing angle; y=100μm)

Towards Dense Form-Factor Integrated Optics:
i) Small Angle X-couplers

Price competition and miniaturisation provide powerful incentives for engineers to seek higher device densities in integrated optics. The ability to cross and overlap channel waveguides with minimal loss or distortion of the guided mode is one route towards achieving this, and a process for which direct UV writing is ideally suited. One such structure, the X-coupler (Fig. 2), comprises of two channel waveguides that intersect at a given angle. They are found in many functional integrated optical devices such as switches, power dividers and wavelength selective splitters. Fabrication of small angle (<5°) ridge-style X-couplers in silica-on-silicon using photolithography and etching are prone to under-etching and step coverage problems. This tends to result in high insertion loss and polarisation sensitivity.

In recent work, we have demonstrated small-angle (0.8°-5°) direct UV-written X-couplers with maximum and minimum coupling ratios of 95% (±0.8%) and 1.9% (±1%) respectively. These structures display very low polarisation and wavelength dependence with typical excess loss of 1.0dB (±0.5dB). Device modelling using BPM and an analytical model showed good agreement with experimental results over a broad crossing angle and wavelength range. Such performance owes itself to UV writing overcoming the aforementioned fabrication issues by allowing smooth crossings with arbitrarily small angles. However, the most significant advantage of our technique is the ability to achieve an index increase in the waist region due to repeated illumination. This additional control over the localised index is necessary to produce a raised waist index for near lossless X-coupler operation [7]. This is graphically represented in Fig. 2.

Fig. 3 shows the coupling ratio behaviour of the X-couplers as a function of crossing angle, wavelength and polarisation. Coupling ratio is defined as the ratio between the coupled power and total output power. These results highlight the advantages of UV multi-exposure in fine-tuning device performance. However, little is known about the photosensitivity behaviour of regions within the immediate vicinity of an earlier UV exposed area, a feature known as the 'proximity effect'. In the following section, we will present the use of planar Bragg gratings in quantifying this proximity effect and also in determining core layer flatness of a novel flat fibre sample.

Planar Bragg Gratings as an Assessment Tool:
i) Quantification of the Proximity Effect

When a channel waveguide structure is defined into a photosensitive substrate using a UV beam, the photosensitive area around the channel can also be affected. As such, an accurate understanding of these local proximity effects in UV writing is critical for development of both complex coupling structures and high density devices.

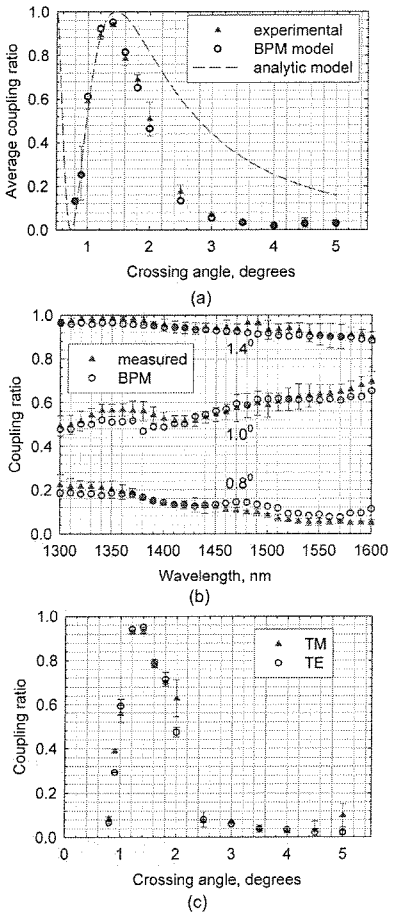

Fig: 3 (a) Coupling ratio against crossing angle (the analytical model is only valid for angles < 1° [7]); (b) Wavelength dependency of X-couplers for 3 different crossing angles showing low dependence over 300nm; (c) Low polarisation dependence of the X-couplers

In current work we have discovered that local photosensitivity increase is evident for regions within 9μm away from the initial exposure with a maximum effective index increase of 8.3×10^{-4}. This quantitative data was achieved through series of experiments, each using sets of three 1mm long Bragg gratings with three different periods (Λ_1=529.3, Λ_2=534.5, Λ_3=539.6nm) defined at a fixed spacing from a set of earlier UV exposed regions. This experimental layout is illustrated in Fig. 4(a), where 'fluence' is the expression for the energy exposed to the sample during the UV writing process.

Reflection spectra of the gratings were recorded, allowing calculation of the average effective index of the waveguide, as depicted in Fig. 4(b). It can be seen that an increase in index is obtained in regions up to 9μm away, highlighting the proximity effect, and with a maximum increase obtained when the same region is multi-exposed (0μm spacing). Effective index increases as large as 8.3×10^{-4} (with respect to the reference gratings) were recorded. We believe

that the behaviour exhibited is either due to non-localised heating effects or more likely a result of diffusion of hydroxyl (OH) species resulting in redistribution of oxygen deficient defects, and therefore an increase in photosensitivity.

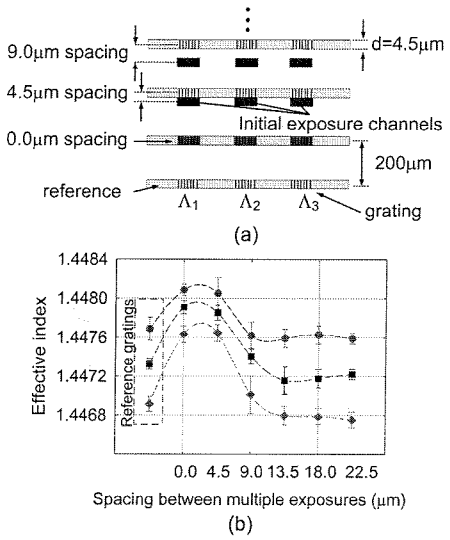

Fig: 4 (a) UV-written Bragg gratings and earlier defined channels for proximity effect characterisation (d: waveguide width); (b) Effective index at various spacing and fluence values (●: Fluence, $F = 22\text{kJcm}^{-2}$, ■ : $F = 14\text{kJcm}^{-2}$, ◆ : $F = 9\text{kJcm}^{-2}$)

ii) Assessment of Flat-Fibre Core Layers

While integrated optical devices in silica-on-silicon offer dense functionality in a robust package, they are rarely considered compatible with the fields of remote or distributed sensing or long-haul one-dimensional fibers. At the ORC we aim to change that with the development of new 'flat-fibers' that combine the advantages of existing low-cost fiber drawing with the functionality of planar lightwave circuits in a novel hybrid format (Fig.5). Adapted from MCVD fiber fabrication, our preforms are deposited and collapsed into a rectangular geometry before drawing, resulting in extended lengths of mechanically flexible flat-fiber material with a photosensitive germanium-doped planar core. By taking this approach, we hope to extend beyond the centimeters-length limitations of traditional planar substrates to allow exotic material compositions, integrated optical device layouts, and local sensing functions to be distributed over extended distances with no coupling or compatibility concerns.

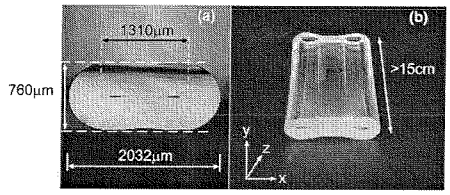

Fig: 5 (a) Cross section; and (b) perspective views of the novel flat fibre sample

In order to optimise the flat-fibre substrates for use in integrated optics, physical and optical assessment in terms of layer flatness and waveguide birefringence must be performed. UV writing again provides a useful approach to this problem, allowing a series of identical Bragg gratings to be inscribed and assessed across the sample profile. Using direct grating writing through the ~350μm thick cladding layer of early samples, a series of Bragg gratings were written into the core of the planarised fibre at 100μm spacing to allow comparative assessment across the flat core region. Inherently, maintaining the overlap and interference pattern of the two focussed 4μm spots places a stringent need for the core layer to be flat and uniform if channel waveguides and Bragg gratings are to be properly defined. Despite the 'bow-tie' profile of our early samples, planar gratings have been successfully demonstrated to prove that the core layer is uniform along the direction of propagation. The reflection spectrum from the first flat-fibre sample with integrated planar Bragg grating developed at the ORC is shown in Fig.6, as was recorded using an ASE source and optical spectrum analyser via a 3-dB coupler. The inset shows the grating reflection and the ASE spectra from the source.

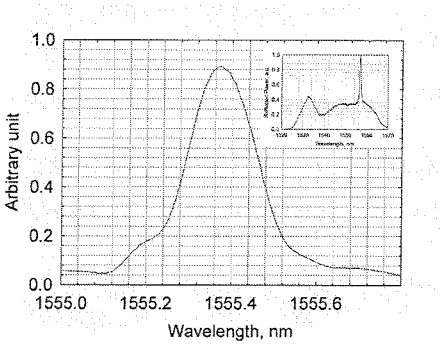

Fig: 6 First demonstration of Bragg reflection in flat fibre sample. The inset shows the ASE spectra of the input light and the Bragg gratings reflection

Following this initial success we proceeded to fabricate identical gratings along the cross section of various flat fibres, allowing us to determine the lateral surface uniformity of each sample. Here, any thickness variation will affect the effective index value of the fabricated structure with a resultant shift in Bragg wavelength. This process also allows us to derive the birefringence of the sample by successively launching TE and TM polarised light. Fig. 7 shows the effective index of the fabricated gratings along the sample profile along with the position of each grating.

In this case, Bragg gratings 6 and 7 display multi-mode behaviour, attributed to the increase in core thickness as we approach the edge of the sample. We have obtained an average birefringence of $3.3\text{x}10^{-4}$ from the same experiment and we believe this low birefringence is due to the reduced level of inter-layer stress-induced birefringence, which is common

in conventional silica-on-silicon samples. Using direct UV writing and planar Bragg gratings in this way highlights the applicability of this process as a material assessment and design tool.

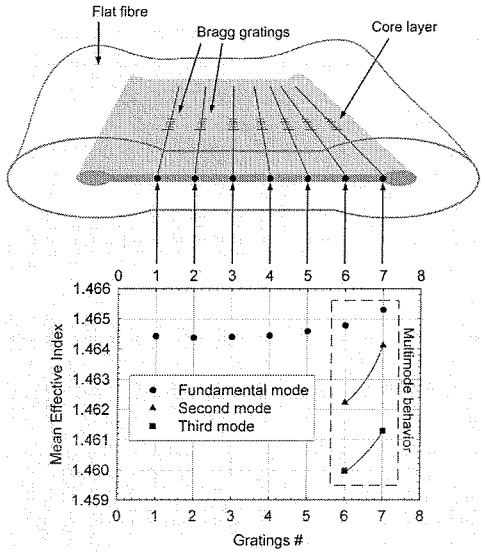

Fig: 7 Mean effective refractive index variation across the cross section of the sample core layer. Gratings 6 and 7 exhibit multi mode behaviour as the core layer thickness increases approaching the edge (solid lines are for indicative purpose only)

Application-based Devices:

i) Tunable Liquid Crystal Gratings

Reconfigurable integrated optical devices are essential in today's dense and complex telecoms meshes. A commonly employed component to fulfill this requirement on the silica platform is a planar Bragg grating, where the ability to tune the reflection peak represents a key enabler towards realizing an all-optical dynamic network. Our approach to this important area of commercial interest has been the development of a series of electrically tunable liquid crystal Bragg gratings devices, which offer up to 114GHz of tunability at just 170Vpp voltage.

Based on a direct-UV-written channel waveguide with an etched window above a planar Bragg grating, these devices operate by use of evanescent coupling into an electrically tuned nematic liquid crystal. Such electrically tunable devices work on the principle of shifting the Bragg wavelength by modifying the effective index of a waveguide in a multilayer substrate. This is achieved by overlaying the grating with a liquid crystal that features a refractive index anisotropy that can be electrically manipulated. Modifying the liquid crystal refractive index subsequently alters the effective index of the waveguide, leading to Bragg wavelength shift. Fig. 8 depicts the schematic diagram of the assembled device and an example Bragg tuning curve.

The demonstrated Bragg wavelength tuning over multiple telecoms channel spacing electrically is encouraging, and our development of a cascaded architecture of such integrated liquid crystal devices operating at different Bragg wavelengths could pave the way towards true colorless add/drop modules for dynamic dense optical networks.

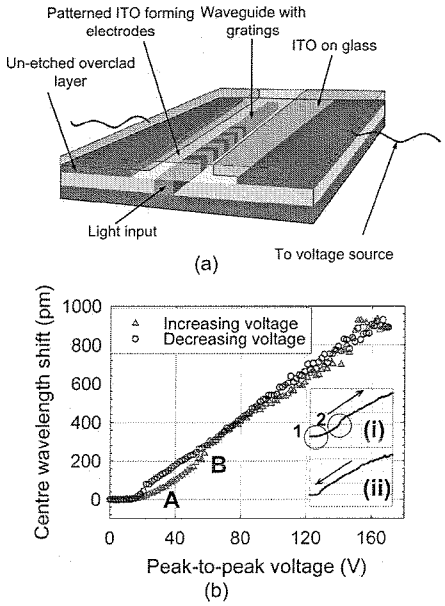

Fig: 8 (a) Schematic diagram of liquid crystal Bragg grating configuration; (b) Tuning curve with insets showing the threshold points

Conclusions

Discussed are our most recent activities in the field of novel direct-UV-written integrated optical devices. The use of direct-UV-written planar Bragg gratings in assessing important physical and optical parameters of various material structures, such as photosensitivity proximity effects and core layer thickness, is presented along with a novel flat optical fibre geometry designed for distributed lab-on-a-chip applications. Ongoing work in the design and optimization of UV-written electrically tunable Bragg gratings for use in reconfigurable optical networks will also be presented.

References:

[1] E. A. Chandross et al *Applied Physics Letters*, vol. 24, pp. 72-4, 1974.

[2] M. Svalgaard et al *Electronics Letters*, vol. 30, pp. 1401-3, 1994.

[3] M. Svalgaard and M. Kristensen *Electronics Letters*, vol. 33, pp. 861, 1997.

[4] M. Svalgaard *Electronics Letters*, vol. 33, pp. 1694-5, 1997.

[5] C. B. E. Gawith et al *Applied Physics Letters*, vol. 81, pp. 3522-4, 2002.

[6] G. D. Emmerson et al *Electronics Letters*, vol. 38, pp. 1531-2, 2002.

[7] F. Durr and H. Renner *Journal of Lightwave Technology*, vol. 23, pp. 876, 2005.